

Attribution of climate forcing to economic sectors

Nadine Unger^{a,b,1}, Tami C. Bond^c, James S. Wang^d, Dorothy M. Koch^{a,b}, Surabi Menon^e, Drew T. Shindell^a, and Susanne Bauer^{a,b}

^aNational Aeronautics and Space Administration (NASA) Goddard Institute for Space Studies, New York, NY 10025; ^bCenter for Climate Systems Research at Columbia University, New York, NY 10025; ^cUniversity of Illinois, Urbana-Champaign, Urbana, IL 61801; ^dEnvironmental Defense Fund, New York, NY 10010; and ^eLawrence Berkeley National Laboratory, Berkeley, CA 94720

Edited by A R Ravishankara, NOAA Earth System Research Laboratory, Chemical Sciences Division, Boulder, CO 80305, and approved December 22, 2009 (received for review June 11, 2009)

A much-cited bar chart provided by the Intergovernmental Panel on Climate Change displays the climate impact, as expressed by radiative forcing in watts per meter squared, of individual chemical species. The organization of the chart reflects the history of atmospheric chemistry, in which investigators typically focused on a single species of interest. However, changes in pollutant emissions and concentrations are a symptom, not a cause, of the primary driver of anthropogenic climate change: human activity. In this paper, we suggest organizing the bar chart according to drivers of change—that is, by economic sector. Climate impacts of tropospheric ozone, fine aerosols, aerosol-cloud interactions, methane, and long-lived greenhouse gases are considered. We quantify the future evolution of the total radiative forcing due to perpetual constant year 2000 emissions by sector, most relevant for the development of climate policy now, and focus on two specific time points, near-term at 2020 and long-term at 2100. Because sector profiles differ greatly, this approach fosters the development of smart climate policy and is useful to identify effective opportunities for rapid mitigation of anthropogenic radiative forcing.

global warming | mitigation | air pollution | ozone | aerosols

Carbon dioxide (CO₂) is the most important single contributor to global climate change and therefore mitigation policies and actions must focus on this species even though impacts may take decades to be realized. The committed air pollutants tropospheric ozone (O₃) and fine aerosol particles also significantly affect global climate but in complex ways involving both warming and cooling (1). These air pollutants, hereafter referred to as short-lived species (SLS), have short atmospheric lifetimes of days to weeks such that changes in their precursor emissions will have a swift change in radiative forcing. Their combined climate forcing effect since preindustrial times may outweigh that of CO₂ (2). Concerns about the rapid rate at which climate is changing at present place urgent emphasis on exploiting the potential benefit of SLS (especially O₃ and black carbon) reductions in global climate change. The ability to evaluate these benefits is somewhat confounded by the committed aerosols that cool the climate, complex interactions between gas and aerosol pollutants, and the lack of useful metrics for air pollutants with uneven spatial distributions.

O₃ is a greenhouse gas that warms the atmosphere. Most fine aerosol particles, including sulfate, nitrate, and organic carbon, scatter solar radiation back to space and lead to cooling, except for black carbon, which absorbs solar radiation and warms the atmosphere. Aerosols also affect climate by modifying the properties of clouds. Hygroscopic aerosols that serve as efficient cloud condensation nuclei can increase cloud droplet number concentrations (CDNC) and reduce cloud droplet effective sizes (R_{eff}) if cloud liquid water content remains unchanged (3)—the first indirect effect. A consequence of smaller droplet sizes is that they do not grow large enough to participate in cloud droplet coalescence processes, inhibiting precipitation formation and increasing cloud liquid water path (LWP) and cloud lifetime (4)—the second indirect effect. The absorbing black carbon aerosol has additional climate effects though solar heating of the boundary

layer that leads to the evaporation of clouds—the semidirect effect (5) and changes in snow albedo that are highly uncertain. The combined direct and indirect effects of aerosols exert a net cooling that may be masked about 50% of the global warming by greenhouse gases (6, 7).

O₃ is not emitted directly, but is formed in the atmosphere by complex nonlinear chemical production and loss processes that are variable in space and time. The O₃ budget involves a stew of gaseous species, including carbon monoxide (CO), methane (CH₄), nonmethane volatile organic compounds (NMVOCs), nitrogen oxides (NO_x), water vapor, as well as aerosols and sunlight. Sulfate and nitrate aerosols are also intimately linked to O₃ photochemistry because they are formed from the precursor gases SO₂, NH₃, and NO_x with rates that depend upon the availability of key tropospheric oxidants. As well as being an O₃ precursor, CH₄ is itself an important greenhouse gas (2) but has a considerably longer lifetime than the SLS, around 9–10 yr in the troposphere. At the same time, O₃ precursor emissions impact CH₄ indirectly through changing the CH₄ lifetime. CO and NMVOC emissions tend to reduce oxidation capacity and thus increase the CH₄ lifetime. NO_x emissions tend to increase oxidation capacity and thus decrease the CH₄ lifetime. The changes in CH₄ induced by SLS precursors will also affect O₃ on the longer time scale of the CH₄ lifetime (8). Each human activity or economic sector emits a multifarious portfolio of these precursor gases and aerosols simultaneously. Each sector also emits long-lived greenhouse gases (LLGHG) that may reside in the atmosphere for decades to centuries including carbon dioxide (CO₂) and nitrous oxide (N₂O); these gases are most traditionally associated with climate change, but they operate on different timescales.

O₃ and fine aerosols are currently controlled by air quality legislation without consideration of their effects on climate. The significant health and economic rewards of abating air pollution are becoming increasingly evident. Eliminating aerosols alone would likely exacerbate climate warming by exposing the Earth system to the full impacts of the greenhouse gases. Policymakers are beginning to consider the benefits of synergies between climate change, energy, and air quality management policies (9). While air quality impacts are frequently considered for climate change policies, the climate effects of air pollutants are not usually considered in air quality policies.

The radiative forcing (RF) concept has been designed to quantify human and natural influences on the climate system and is defined as the net energy flux difference at the top of the atmosphere (TOA) caused by an imposed change in the pollutant loading relative to an unperturbed initial state. The

Author contributions: N.U. designed research; and N.U. performed research; and N.U., T.C.B., J.S.W., D.M.K., S.M., D.T.S., and S.B. analyzed data; and N.U. wrote the paper.

The authors declare no conflict of interest.

This article is a PNAS Direct Submission.

Freely available online through the PNAS open access option.

¹To whom correspondence should be addressed. E-mail: nunger@giss.nasa.gov.

This article contains supporting information on-line at www.pnas.org/cgi/content/full/0906548107/DCSupplemental.

Intergovernmental Panel on Climate Change (IPCC) bar chart (2) (Fig. 2) quantifies the RF in terms of changes to single species between the present day and the preindustrial atmosphere (1750). RF is related to the global mean equilibrium surface temperature response via climate sensitivity. Here, we continue the evaluation of RF as an indicator of climate impact, although we acknowledge that it is imperfect in that regard (10–12).

We now reexamine the traditional focus of the IPCC—and indeed, of the entire climate science community—on RF by individual species and their changes since preindustrial times. This conventional presentation obscures both the multipollutant nature of activity change and potential interactions between different chemical components. Thus, it may not foster the development of smart climate policy, because it ignores the possibility that mitigation actions can affect multiple SLS with opposing or enhancing climate impacts (13). Recent research has begun to quantify RF according to human activity or economic sector (e.g., 14–19). This unique approach inherently includes chemical couplings between the species emitted from one sector. Previous studies have typically considered only one particular activity, or only either gaseous or aerosol effects, or only SLS or LLGHG. A full sector-based assessment that considers all activities and forcing agents is needed. Furthermore, in contrast to the historical perspective that is used by the IPCC to diagnose climate change since the industrial revolution, we adopt a forward-looking perspective based on current emissions that is most relevant for the development of environmental policy aimed at effective mitigation of anthropogenic RF.

Halocarbons (CFCs, HCFCs, halons, PFCs, and HFCs) and other halogenated compounds (SF_6) are important climate warmers and are associated with an RF of similar magnitude to O_3 ($+340 \text{ mWm}^{-2}$). However, these compounds originate from specific industrial sources that are typically different than O_3 and aerosol precursors. HFCs, PFCs, and SF_6 are already included in the Kyoto Protocol and CFCs and HCFCs are addressed in the Montreal Protocol. Therefore, we do not consider them in this study and focus our attention on the climate effects of O_3 , fine aerosols and coemitted LLGHGs from fuel burning, and agricultural and waste activities. In the present analysis, we do not consider some of the smallest indirect RF impacts, for example oxidation of CH_4 to CO_2 and the impacts of CH_4 on stratospheric water vapor. Furthermore, we do not evaluate RFs due to atmosphere-ecosystem feedbacks including the indirect impacts of O_3 and aerosols on the land carbon sink (20, 21), or impacts of aviation emissions on contrails and cirrus clouds, although we do acknowledge that these indirect effects may be potentially substantial.

Procedures

Here we present a consistent and comprehensive multipollutant assessment of the total RF due to emissions from the 13 major anthropogenic economic sectors. The SLS are removed from the atmosphere in days to weeks, thus their atmospheric concentrations are determined entirely by the current emissions and their sectoral RF remains the same (for constant emissions) into the future. In contrast, the LLGHGs persist in the atmosphere for decades to centuries. Therefore, assessment of the future impacts of current emissions must take into account the buildup of LLGHGs over time. Similarly, the LLGHG atmospheric concentrations, and therefore RF, will respond on these longer time scales to removal of emissions from a particular sector. There is already an accumulation of LLGHGs in the atmosphere that is due to past emissions from the different sectors throughout history. We choose to reset the anthropogenic clock to zero at year 2000.

We calculate the instantaneous RF due to perpetual constant year 2000 emissions from each sector under present atmospheric conditions and taking into account the accumulation of the

LLGHGs since 2000. RF values are reported every 5 yr for the next 100 yr up to 2100. The values also represent the total RF change that would occur if the sector were turned off now, but are of the opposite sign so that sectors that have a net positive RF would lead to global cooling when the emissions are switched off and vice versa. This approach is useful for identifying actions that enable the most rapid reduction of RF. The large difference in atmospheric lifetimes between the SLS, CH_4 and the LLGHG necessitates the use of two different models to determine the RFs. Attribution of direct RF by SLS (O_3 , sulfate, nitrate, black carbon, and organic carbon) to each sector is calculated using the NASA Goddard Institute for Space Studies (GISS) atmospheric composition-climate model (22), details of which are included in the *SI Methods* section. The O_3 RF due to the SLS precursor emissions is denoted “S- O_3 ”. RF due to the effects of aerosols on clouds that includes the first and second indirect effects and semidirect effects (but not black carbon effects on snow albedo), collectively referred to here as aerosol indirect effect (AIE), is also calculated on-line in the atmospheric composition-climate model (23). Further details of the AIE simulation are in *SI Methods*. The sectoral RF contributions by direct methane emissions (“D- CH_4 ”) and the LLGHG emissions (CO_2 and N_2O) are calculated using the gas-cycle component of the Model for the Assessment of Greenhouse-gas Induced Climate Change (24). The indirect chemical effects of the SLS precursor emissions that impose a CH_4 RF through influencing the CH_4 lifetime (denoted “I- CH_4 ”) are calculated as described in *SI Methods*. Both direct and indirect CH_4 changes also affect O_3 on the longer time scale of the CH_4 lifetime. We quantify this secondary O_3 RF (denoted “M- O_3 ”) as described in *SI Methods*.

We do not incorporate potential future changes in emissions because of the large degree of uncertainty in future emissions projections (25, 26). Our main goal is to inform effective policies and therefore it is critical that our results are based on current activities in the real atmosphere, although the results may serve as a useful guide to the impacts of future policies. The instantaneous RF for sustained emissions is essentially the same as the integrated RF for pulse emissions that is used to develop the Global Warming Potential metric for different time horizons (2).

Emissions. We use an emission inventory for the year 2000 (27) that provides data for all precursor emissions except black and organic carbon emissions from (28), with updated energy use data and updated emission factors. Biomass burning emissions are 1997–2002 averages from the Global Fire Emissions Database (29). NH_3 emissions are from the Edgar 2.1 inventory representative of the year 1990 due to the lack of more recent data. The emissions are partitioned into 13 explicit sectors defined in *Table S1*. The power sector incorporates all energy production activities including CH_4 from coal mining, oil and gas production and handling. The agriculture sector includes rice cultivation. Biomass burning for the SLS precursors includes all burning types (tropical, savannah, and shrub fires, also middle and high latitude forest and grassland fires). CO_2 emissions are considered to be sustainable for all biomass burning sources except tropical deforestation. The fraction of unsustainable (nonrenewed) CO_2 emission from household biofuel burning is assumed to be 10%.

Climate Impacts of Short-Lived Species by Sector. A detailed breakdown of the SLS and AIE RFs is given in *Table S2*. The largest individual effects ($\sim 200 \text{ mWm}^{-2}$) are imposed by sulfate aerosol from the power and industry sectors and carbonaceous aerosols from biomass burning. The ratio of black carbon to organic carbon RF is important since these species are usually emitted together but have RF of opposite sign. The organic carbon RF for biomass burning is about twice as large as the black carbon RF from this sector, even though this activity gives the largest single black carbon RF. Additional substantial black and organic carbon

RFs are from on-road transportation, household biofuel, and industry. Of these activities, the black carbon RF always dominates over the organic carbon RF, but the ratio is notably highest for on-road transportation and lowest for household biofuel.

The power and industry sectors yield positive nitrate RF indicating that these sectors lead to a net global reduction in nitrate aerosol. These sectors are the two major anthropogenic sources of SO₂ emissions and hence contributors to sulfate formation. Sulfate and nitrate essentially compete for available NH₃, however, sulfate has the advantage due to preferential neutralization and the lower vapor pressure. Therefore, in the case of the emissions mix from the power and industry sectors, ammonium sulfate is formed at the expense of ammonium nitrate and the effect appears to outweigh additional nitrate formation due to coemitted NO_x from these activities.

Aerosols from the industry, power, and biomass burning sectors are efficient at increasing CDNC (~10% globally) thereby reducing R_{eff} (~ -1% globally). In the case of the power and industry sectors, these microphysical changes result in increases in low and total cloud cover (~0.02%), liquid water path (~0.24 gm⁻²), and cloud optical depth (~0.4-0.5) that act to enhance reflectivity and result in an AIE RF of up to -200 mWm⁻². For biomass burning that takes place predominantly in the tropics, the enhanced AIE RF is mainly due to increases in cloud optical depth (~0.23) since impacts on cloud cover and liquid water path are negligible at the global scale (although substantial in the tropics). Aerosols from the on-road transportation and household biofuel sectors cause much smaller global increases in CDNC (~1%) and decreases in R_{eff} (-0.3%) since the majority of these aerosols are carbonaceous and do not participate in cloud nucleation processes as effectively as sulfates and nitrates. Cloud optical depth changes are somewhat negligible. For the on-road transportation sector, both low and total cloud cover actually decrease (~ -0.1%) leading to positive AIE RF, which we ascribe to semidirect effects driven by the large black carbon component of the aerosol mix. A similar situation occurs for the household biofuel sector, although here low cloud cover increases, whereas total cloud cover decreases such that changes in cloud redistribution appear to be dominating over the other indirect effects. In general, on global scales, aerosol impacts from the other individual sectors were not large enough in the model to drive significant AIE RF relative to internal climate variability.

S-O₃ RFs are in general much smaller than aerosol effects. Biomass burning provides the largest S-O₃ RF and additional important sectors are on-road transportation and household biofuel. The NH₃ emissions from the agriculture and animals sectors result in small negative S-O₃ RF due to NO_x being sequestered in nitrate aerosol formation.

Climate Impacts of CH₄ and Long-Lived Greenhouse Gases by Sector.

A breakdown of the CH₄-related and LLGHG RFs by sector are provided in Table S3 and Table S4, respectively. For the LLGHGs values are presented for time points 2020 and 2100. The largest CH₄ effects are by D-CH₄ from power, animals, agriculture, and landfill/waste. Of these sectors, only power has an important negative I-CH₄ RF which counteracts ~15% of the D-CH₄. The domestic biofuel sector has approximately the same magnitude and sign D-CH₄ and I-CH₄ whereas for the industry sector the I-CH₄ is negative and outweighs D-CH₄. Shipping and aviation sectors have negligible D-CH₄ but modest cooling effects through I-CH₄. M-O₃ is larger than S-O₃ RF for several key sectors (power, agriculture, animals, and waste/landfill). CO₂ provides the largest individual RFs with the major contributions from the fossil fuel sectors (industry, power, household fossil fuel, and on-road transportation). The CO₂ RFs are of the same magnitude as the largest direct aerosol RFs in the near-term but increase to about three times the magnitude on longer time scales. Substantial

N₂O RF is associated with agriculture and animals while other sectors are unimportant for this agent.

Synthesis: Climate Impacts of Current Emission Sectors. We present the future RF from year 2000 emissions at time points 2020 (Fig. 1A) and 2100 (Fig. 1B) grouped by sector. The largest net near-term negative RFs are from the biomass burning and industry sectors due to substantial cooling effects from scattering aerosols and their impacts on clouds. Similarly, the power sector has a large cooling component through aerosols but the large CO₂ emission from this sector results in a net positive RF. On-road transportation and household biofuel exert the largest net positive RF in the near-term. For on-road transportation, the sum of the SLS effects is about the same as the CO₂ effect. Animal husbandry and waste/landfill, sectors with the largest D-CH₄ RF but zero CO₂ effects, are amongst the largest net warming activities in the near-term. The aviation sector has the smallest RF across all the human activities (consistent with the smaller fuel use relative to other activities). Here we do not include the effects of aviation emissions on contrails and cirrus clouds. The IPCC estimates a RF of +10 mWm⁻² for the contrail effects (2), although the impacts of aviation emissions on cloudiness are highly uncertain. Aviation RF effects will be discussed further in a separate paper. Shipping has a net cooling effect, again the CO₂ RF is dominated by the SLS RF. While this sector has insignificant AIE in the present model, other studies suggest much larger AIE (30).

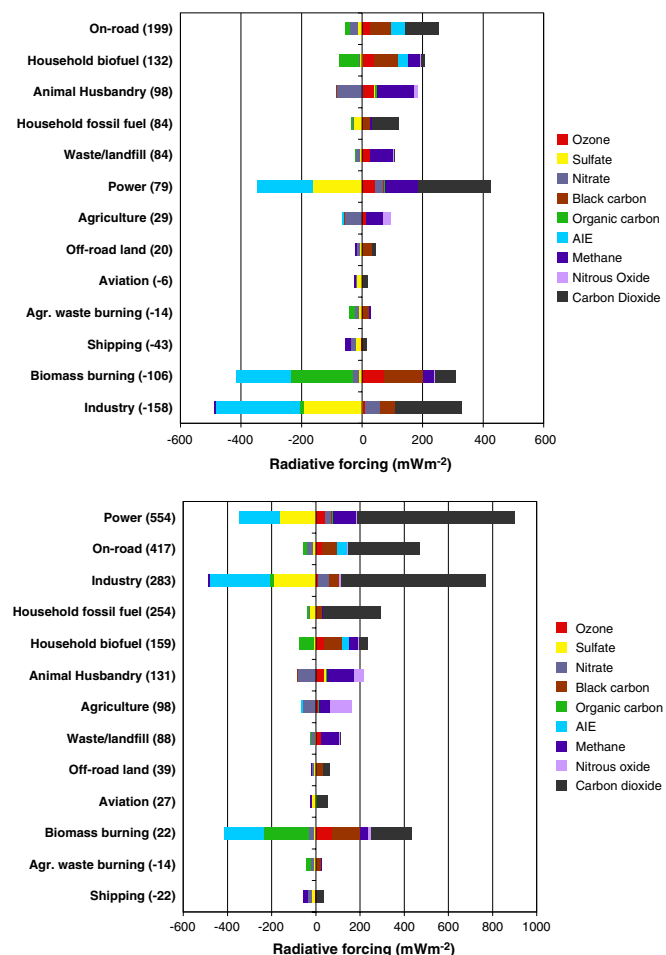


Fig. 1. Radiative forcing due to perpetual constant year 2000 emissions grouped by sector at (a) 2020 (b) 2100 showing the contribution from each species. The net sum of total radiative forcing is indicated by the title of each bar. A positive RF means that removal will result in climate cooling and vice versa.

At 2100, a different picture emerges as the LLGHG RF effects become more important. Now, power has the largest net positive RF and industry changes sign to be strongly positive. Net RF from on-road transportation doubles. Biomass burning becomes somewhat climate neutral with a weak positive RF. Household fossil fuel has about the same net positive RF as industry but with a much smaller cooling component from scattering aerosols. The net RF from household biofuel is about the same for the near and long-term time horizons. Only agricultural waste burning and shipping exert net negative RF on the longer time scale and the effects are somewhat weak. Substantial positive RFs are from the CH₄ dominated sectors (animals, agriculture, and waste/landfill). The net RF from agriculture triples from the near-term to the long-term due to N₂O effects.

The future evolution across the coming century of the total RF including all agents (SLS, CH₄, and LLGHG) by each current emission sector is shown in Fig. 2. Dramatic profile changes occur for the industry, power, and biomass burning sectors whose large aerosol cooling ($> -200 \text{ mWm}^{-2}$) is offset by CO₂ warming at different rates depending on the balance of those emissions. For power, the RF rapidly becomes positive in about 10–15 years, for industry the RF becomes positive in midcentury, whereas for biomass burning the net RF does not become positive until much later at 2070. For sectors dominated by CH₄ effects (animal husbandry and agriculture) the RF increases for about 10–15 years and then levels off to a constant value. On-road transportation and household biofuel burning have the largest positive RF initially. The household biofuel RF value remains relatively constant throughout time because the effects are dominated by the SLS (non-CO₂) agents. The on-road transportation RF continues to grow and remains the largest positive RF until midcentury when it is superseded by the power sector.

Uncertainties in RF by Sector. Uncertainties in modeled RF include model representation of the physical, chemical, and optical processes and internal variability in the climate model. The fractional uncertainties in sectoral RF from these causes are similar to the fractional uncertainty due to all emissions. We focus the uncertainty analysis on the 2020 time point. Table S5 shows the SLS RF uncertainty due to climate model internal variability that is based on the standard error of the mean from 10 yr of model output (included as a percentage of the total sector RF). Larger uncertainty occurs for sectors that have an AIE RF and/or large SLS/LLGHG ratio where the SLS are mostly O₃ and aerosols, not

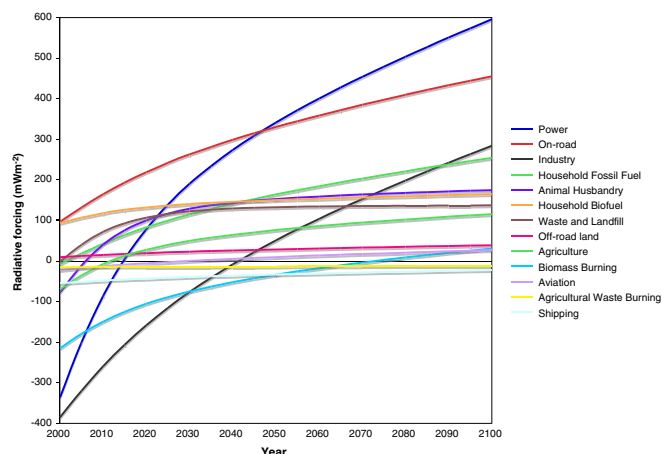


Fig. 2. Summary of the future evolution over the coming century of total radiative forcing (including SLS, AIE, CH₄ and LLGHGs) due to perpetual constant year 2000 emissions by sector. The SLS and AIE values remain constant across the time period. A positive RF means that removal will result in climate cooling and vice versa.

CH₄. The emission rate in each sector is another uncertainty; this affects the magnitude but not the sign of each estimated RF, and Table S5 also estimates this fractional value for the SLS RF based on uncertainties in the magnitude of black carbon and organic carbon (28), which is expressed as a percentage of the sectoral total RF. Finally, uncertainties in the composition of SLS or their precursors could affect the sign of the RF from each sector if the species have opposing RF. Quantitative uncertainties do not exist for most emission inventories and therefore we cannot estimate the confidence interval caused by uncertainties in sectoral profiles. However, Table S5 indicates (using “**”) those sectors that emit species with opposing RF and high uncertainties. Compared to other sectors, the on-road transportation and power sectors are more certain based on this analysis. The sectors that have the largest uncertainties and/or for which the net sign of the RF is least robust are household biofuel, industry, off-road transportation, agricultural waste burning, biomass burning and shipping.

Comparison of Short-Lived Species’ RF with IPCC Estimates Because the SLS atmospheric concentrations are dependent on current emissions only, summing over the sector-based RFs calculated in this work for each individual species, gives RF values that are equivalent to the IPCC assessment approach and we compare corresponding values in Table S6. RF by CH₄, O₃, total direct aerosol effects, direct sulfate, and direct black and organic carbon from fossil fuel sources calculated in this study are in close agreement with the IPCC values. A discrepancy occurs for the direct biomass burning aerosol RF estimate. In this study we present RFs due to emissions from the entire biomass burning emission source, whereas in the IPCC estimate, assumptions have been made about the preindustrial level of biomass burning emissions relative to the present day source that range from 10% to 50%, depending on the model. Recent work suggests that biomass burning emissions may have even been larger in the preindustrial atmosphere than present day (31). For the AIE, the IPCC value includes only the cloud albedo effect, whereas here we also include cloud lifetime and semidirect effects. The direct nitrate RF is higher by about a factor of 2 than IPCC, which is most likely related to the use of on-line oxidants in this study.

Spatial Pattern of RF from Current Emissions at 2100. Fig. 3 shows the net sum of instantaneous RF at 2100 by LLGHG, CH₄ effects and direct SLS RF (but not AIE) for several of the key sectors. Sectors that have substantial effects from SLS (e.g. biomass burning) drive more variability in the spatial pattern of RF versus sectors that are dominated by LLGHGs (e.g. household fossil fuel). The large net positive RF from power and industry is distributed worldwide. However, the LLGHG warming is substantially dampened for these sectors over industrialized regions (mostly in the northern hemisphere) due to cooling by aerosol, even after 100 yr accumulation of CO₂. A result is that power has a larger net positive RF in the southern hemisphere than the northern hemisphere. On-road transportation and household fossil fuel also have substantial net positive RF worldwide. The net positive SLS RF from the on-road transportation sector substantially enhances the LLGHG RF in the northern hemisphere. Power, industry and on-road transportation contribute the largest warming in the Arctic region. Local net positive RF from household biofuel over East Asia and North Africa that is due to SLS effects alone is of similar magnitude to the warming effects from power, although the latter are spread over much larger regions. The largest local net negative RFs ($\sim -2000 \text{ mWm}^{-2}$) occur over South America and Central Africa due to biomass burning. Local net negative RFs (up to -1000 mWm^{-2}) also occur over East Asia due to power and agriculture, and Europe due to animal husbandry. Understanding the global and regional climate responses to these localized RFs is an important emerging future research direction.

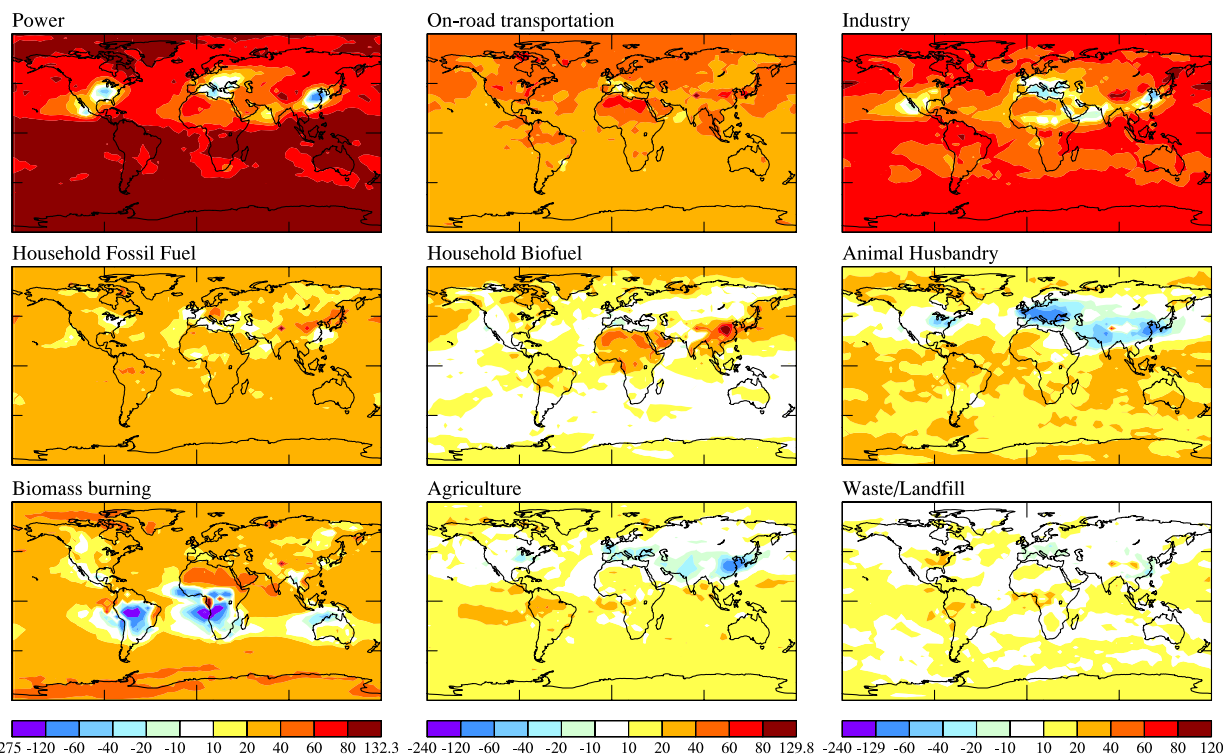


Fig. 3. Spatial distribution of the net sum of the future instantaneous radiative forcing at 2100 by short-lived species (O_3 , sulfate, nitrate, black carbon, organic carbon), CH_4 direct and indirect effects and LLGHGs (CO_2 and N_2O) due to perpetual constant year 2000 emissions by sector. Units are $\times 100 Wm^{-2}$.

Discussion and Conclusions

We have presented a multipollutant RF assessment of the impact of current emission sectors that identifies the total climate impacts of mitigating a range of different pollutants and activities. The results demonstrate that both the SLS and LLGHG need to be considered in smart climate policy to avoid unintended climate consequences. The decadal-scale climate effects of cooling aerosols need to be included in evaluations of control strategies, especially for actions that affect the power, industry, biomass burning, and shipping sectors. The sectoral bar chart can be used, for example, to assess the impacts of new technologies on climate, or in tandem with the stabilization wedge approach of Pacala and Socolow (32). The information provided is complementary to the single-species information provided by the IPCC assessments.

If the policy goal is to achieve rapid and immediate reduction in anthropogenic RF, then effective opportunities lie in reducing emissions from the on-road transportation, household biofuel, and animal husbandry sectors. The on-road transportation total RF is fairly robust with uncertainty in the range 20–40% whereas uncertainties are higher for household biofuel (~160%) and animal husbandry (~90%). Reducing emissions from the on-road transportation sector is particularly attractive because this action yields both rapid and longer-term climate benefits. Newly emerging public health research indicates that traffic-related particulate matter is more toxic than inorganic components like sulfate and nitrate from the power sector (33) so reducing emissions from on-road transportation has additional benefits for human health. In order to protect the Earth's climate in the longer-term and tackle concerns about climate change toward the end of this century, then emphasis must be placed on reducing emissions from the power and industry sectors consistent with other findings (34). Total power RF is more robust than for industry (~50–70% versus ~40–120%). Caution must be taken in reducing emissions from the industry sector since this action will considerably accelerate near-term warming. A similar situation would occur for reducing

emissions from biomass burning consistent with previous analyses of this sector (14).

Limitations of the study include uncertainties in the SLS direct and indirect RF that are driven by uncertainties in the model and the emission inventory. We recommend future multimodel studies of sector-based RF, with an eye to understanding how model uncertainties may affect the comparisons presented here. This study is based on present day emissions and therefore assumes the current mix of air pollution controls on the major emission sectors, which are generally effective in the developed world. Future growth in the major sectors is likely to proceed mostly in the developing world. The SLS RF are dependent on emission location, typically the RF efficiency is greater for pollutants emitted in lower latitudes (where insolation and photochemical activity are higher) as opposed to the midlatitudes (e.g. 8, 17). For that reason, the results presented here should not be directly extrapolated to understanding future development and energy scenarios. However, in a previous study, in which we quantified the SLS RF by global sector for a future scenario that features substantial emission reductions in developed countries and rapid economic growth in developing countries, the total SLS sectoral RF values for 2030 were remarkably similar to the values reported here for the power, industry, transportation, and household biofuel sectors (17). At least for that particular future scenario, results are similar for an altered geographic distribution of emissions.

The sectors in the present study are still somewhat broad. Future work will consider even greater detail within sectors, for example power stations that operate with coal or natural gas, heavy and light duty vehicles, and regional sectors. Policy decisions regarding effective mitigation actions also depend upon other critical factors including cost and feasibility.

ACKNOWLEDGMENTS. This research was supported by the NASA Atmospheric Chemistry Modeling and Analysis Program (ACMAP). We thank the NASA Center for Computational Sciences for computing support.

Supporting Information

Unger et al. 10.1073/pnas.0906548107

SI Text SI Methods

We applied the NASA Goddard Institute for Space Studies (GISS) atmospheric composition-climate model described in detail and comprehensively evaluated in (22). Briefly, the model comprises the GISS version ModelE general circulation model (35) with embedded fully interactive photochemistry and aerosol modules. We use 23 vertical layers (model top in the mesosphere) and 4×5 degree latitudinal by longitudinal horizontal resolution. The atmospheric composition-climate model includes full coupling between tropospheric gas-phase and aerosol chemistry (36, 37) and aerosols and cloud microphysics for liquid-phase stratus and cumulus clouds (38). The aerosols are assumed to be externally mixed. The direct instantaneous TOA RF by the SLS is calculated internally within the climate model's radiation scheme (35). We estimate the RF due to AIE from the difference between the net radiation at the TOA and all direct radiative effects (38).

Simulations. In all simulations using the atmospheric composition-climate model, monthly mean sea surface temperatures and sea ice climatologies are prescribed for 1990–1999 (1). Methane concentration is prescribed to hemispherically averaged values (NH = 1,814 ppb and SH = 1,733 ppb) based on observations for the year 2000 (2). A present day control simulation is performed based on the emissions inventory described in the paper and Table S1. In order to quantify the short-lived species (SLS) radiative forcing (RF) attributable to each emission sector, we performed sensitivity simulations in which we removed all emissions from that sector. Each simulation was run for 12 model years; the first 2 years of the simulations are discarded as spin-up and the remaining 10 years are averaged. The contributions to RF by the individual emissions sectors for each SLS are then determined by taking the difference between the control simulation and the simulation with a missing sector. A further simulation was performed in which all sectors were removed simultaneously.

CH₄ RF Due to Indirect Chemical Effects on the CH₄ Lifetime. Indirect CH₄ RF is determined using the method described in ref. 3. First the change in atmospheric CH₄ concentration due to each emission sector is calculated based on the initial change in the CH₄ lifetime in the climate model and accounting for the feedback of CH₄ on its own lifetime. Then the CH₄ RF is calculated using a standard simplified expression based on the steady-state concentration change (4). Both direct and indirect CH₄ changes also affect O₃ on the longer time scale of the CH₄ lifetime. We quantify this secondary O₃ RF (denoted “M-O₃”) using global average sensitivity results from previous multimodel assessment studies (3, 4).

Aerosol Indirect Effect. Aerosol mass concentrations are converted to aerosol number concentrations assuming log-normal distributions and are related to cloud droplet number concentrations (CDNC) through empirical equations. Additionally, effects of changes to cloud cover and turbulence on CDNC are also included. To represent aerosol effects on precipitation, the auto-conversion scheme in the model is modified to include a dependence on droplet size (as well as CDNC and droplet dispersion effects) such that autoconversion is triggered if droplet sizes exceed 14 μm (5). Model simulated aerosol-cloud interactions been evaluated with satellite-based retrievals to constrain the magnitude of the aerosol indirect effect (AIE) (6). Results indicate that the AIE may be overpredicted over the ocean regions due to an underprediction of cloud droplet size and an overprediction of cloud optical depth. Simulated CDNC was found to be within satellite retrieved uncertainty. Over land locations, coincident retrievals of aerosols and cloud properties are not easily available from satellites and thus evaluation of changes to cloud properties from aerosols is more difficult. A more meaningful global evaluation of the AIE is challenging in the absence of global observations of CDNC that serve as the main link between aerosols and cloud properties.

1. Rayner NA, et al. (2003) Global analyses of sea surface temperature, sea ice, and night marine air temperature since the late nineteenth century. *J Geophys Res* 108(D14):4407–4443.
2. Dlugokencky EJ, et al. (2003) Atmospheric methane levels off: Temporary pause or a new steady-state? *Geophys Res Lett* 30(19):1992–1995.
3. Bernsten TK, et al. (2005) Response of climate to regional emissions of ozone precursors: Sensitivities and warming potentials. *Tellus* 57B:283–304.
4. Ramaswamy V, et al. (2001) *Radiative Forcing of Climate Change. In Climate Change 2001: The Scientific Basis. Contribution of Working Group I to the Third Assessment Report of the Intergovernmental Panel on Climate Change* (Cambridge Univ. Press, Cambridge, UK).
5. Rotstajn LD, Liu Y (2005) A smaller global estimate of the second indirect aerosol effect. *Geophys Res Lett* 32:L05708–doi:10.1029/2004GL021922
6. Menon S, et al. (2008) Analyzing signatures of aerosol-cloud interactions from satellite retrievals and the GISS GCM to constrain the aerosol indirect effect. *J Geophys Res* 113:D14522–doi:10.1029/2007JD009442
7. Olivier JGJ, van Aardenne JA, Dentener F, Ganzeveld L, Peters JAHW (2005) Recent trends in global greenhouse gas emissions: regional trends 1970–2000 and spatial distribution of key sources in 2000. *Environm Sci* 2:81–99.
8. Bond TC, et al. (2004) A technology-based global inventory of black and organic carbon emissions from combustion. *J Geophys Res* 109:D14203–doi:10.1029/2003JD003697

Table S1. Global anthropogenic emissions inventory based on Edgar Fast Track 2000 (7, 8); units for CO, NMVOC, SO₂, CH₄, N₂O, and CO₂ are Teragram (Tg) Full Molecular Mass (FMM)/year; units for NO_x and NH₃ are Tg Nitrogen(N)/year; units for black carbon and organic carbon are Gigagram (Gg FMM)/year

Sector	Precursor PreSpecies									
	NO _x	CO	NMVOC	SO ₂	BC	OC	CH ₄	NH ₃	N ₂ O	CO ₂
Industry	6.0	51	33.6	63.2	769	2559	2.7	0.2	0.7	8414
Power	7.8	12	33.3	57.7	22	18	93.9	0.1	0.1	9127
Household fossil fuel	0.9	27	1.2	8.1	453	486	1.7	2.2	0.02	3390
Household biofuel	2.2	237	27.3	3.1	1471	7823	13.8	0	0.2	495
On-road transportation	8.7	186	33.8	3.7	1235	1630	0.9	0	0.1	4276
Off-road (land) transportation	1.8	13	4.6	2.0	588	292	0.008	0	0.003	390
Shipping	2.9	0.1	0.02	7.3	97	136	0.028	0	0.003	428
Aviation	0.7	0	0	0.2	11	0	0.006	0	0.020	654
Agricultural waste burning	0.2	16	2.0	0.2	371	2266	0.8	1.4	0.020	0
Waste/landfill	0.04	4	2.7	0.05	0	0	58.2	2.7	0.3	0
Biomass burning	10.2	507	31.3	2.7	3500	37200	21.2	1.8	0.9	2740
Animals	0	0	0	0	0	0	88.5	21.1	3.2	0
Agriculture	0	0	0	0	0	0	39.4	12.6	6.6	0

Table S2. Global annual average direct RF due to SLS and AIE RF by sector

	Ozone, S-O ₃	Sulfate	Nitrate	Black carbon	Organic carbon	AIE
Industry	14* (3)	-192* (3)	47* (1)	49* (1)	-15* (3)	-275* (49)
Power	7* (2)	-164* (3)	25* (2)	4 (1)	4 (3)	-182* (46)
Biomass burning	60* (3)	-11* (2)	-21* (2)	131* (1)	-203* (2)	-179* (50)
Agriculture	-7* (3)	1 (3)	-59* (2)	-1 (1)	1 (2)	—
Aviation	3 (3)	-17* (3)	-3* (1)	3 (2)	1 (3)	—
Agr. waste burning	1 (2)	-11* (3)	-11* (2)	21* (4)	-19* (2)	—
Household fossil fuel	2 (2)	-26* (5)	-6* (2)	25* (1)	-5* (2)	—
Shipping	3 (2)	-16* (5)	-16* (2)	3 (2)	-3 (2)	—
Off-road land	2 (2)	-10* (4)	-7* (2)	33* (2)	-2 (3)	—
On-road	26* (2)	-14* (2)	-25* (2)	71* (2)	-16* (2)	43* (33)
Household biofuel	21* (2)	-7 (4)	-4* (2)	82* (1)	-64* (2)	32* (30)
Animals	-4 (3)	5 (3)	-83* (2)	-2 (1)	3 (3)	—
Waste/landfill	-2 (2)	-6 (3)	-16* (2)	1 (1)	-1 (3)	—

Values marked with * indicate significance at 95% confidence level and bracketed numbers indicate standard error relative to internal climate variability based on 10 years of model output. AIE RF values are shown only for results with significance at 95% confidence level. Units are mWm⁻².

Table S3. Global annual average RF from methane direct effects (D-CH₄) and indirect chemical effects of SLS precursors on CH₄ lifetime (I-CH₄) and associated secondary ozone RF (M-O₃) (mWm⁻²)

	Direct Methane Emission		Indirect chemical Effect	
	D-CH ₄	M-O ₃	I-CH ₄	M-O ₃
Industry	4	1	-9	-4
Power	128	46	-21	-9
Biomass burning	28	11	6	2
Agriculture	53	19	0.4	0.2
Aviation	0	0	-6	-3
Agr. waste burning	1	0.4	3	1
Household fossil fuel	2	0.8	2	1
Shipping	0.1	0.01	-18	-7
Off-road land	0	0	-4	-2
On-road	1.2	0.4	1.3	0.6
Household biofuel	18	7	24	10
Animals	120	43	2	1
Waste/landfill	78	29	-0.5	0.2
Sum	433	158	-20	-9

Table S4. Global annual average RF by long-lived greenhouse gases due to perpetual constant year 2000 emissions by sector calculated using the MAGICC model at future time points 2020 and 2100 relative to 2000 (mWm⁻²)

	Future impact of year 2000 emissions			
	2020		2100	
	N ₂ O	CO ₂	N ₂ O	CO ₂
Industry	3	219	10	653
Power	0.4	240	1.4	714
Biomass burning	3	68	12	186
Agriculture	26	0	95	0
Aviation	0	16	0	49
Agr. waste burning	0	0	0	0
Household fossil fuel	0	88	0	258
Shipping	0	11	0	32
Off-road land	0	10	0	29
On-road	0.4	110	2	326
Household biofuel	0.6	13	2	38
Animals	12	0	45	0
Waste/landfill	1	0.4	4	2
Sum	46	775	171	2287

Table S5. Uncertainties in sectoral RFs. Total RF by sector at 2020 and 2100 and the ratio of the SLS/LLGHG RF at each time point (SLS includes CH₄). RF uncertainty is given in terms of internal variability in the climate model based on the standard error of the mean for 10 years of model output, and in terms of the emission rate for the SLS, in both cases as a percentage of the total sector RF. Sectors that emit species with opposing RF and high uncertainties are indicated using ''.**

SECTOR	RF at 2020	SLS/LLGHG at 2020	RF at 2100	SLS/LLGHG at 2100	Uncertainty due to internal climate variability at 2020	Uncertainty due to emission rate at 2020	Large opposing uncertainties
Power	79	-0.7	554	-0.2	70%	50%	
On-road transportation	199	0.8	417	0.3	20%	40%	
Household fossil fuel	84	-0.05	254	-0.01	10%	10%	*
Household biofuel	132	8.7	159	3	30%	160%	*
Animal husbandry	98	7.2	131	1.9	10%	90%	
Industry	-158	-1.7	283	-0.6	40%	120%	*
Agriculture	29	0.1	98	0.03	40%	10%	
Waste/Landfill	84	58.9	88	13.7	10%	100%	
Off-road (land) transportation	20	1	39	0.3	70%	60%	*
Aviation	-6	-1.4	27	-0.4	200%	180%	
Agriculture waste burning	-14	N/A	-14	N/A	90%	250%	*
Biomass burning	-106	-2.5	22	-0.9	60%	420%	*
Shipping	-43	-4.9	-22	-1.7	30%	130%	*

